Higgs sector of the Type-II seesaw model at the LHC

Dilip Kumar Ghosh

School of Physical Sciences,
Indian Association for the Cultivation of Science, Kolkata,India

$1^{\rm st}$ Mediterranean Conference on Higgs Physics,Tangier, Morocco
September 23-26, 2019

- Type II Seesaw model.
- Higgs sector of the model.
- Constraints on the model parameters.
- Examine the model prediction at the current and future run of the LHC.
- Summary.

Based on the work: PRD97,115022 (2018)
DKG, Nivedita Ghosh, Ipsita Saha, Avirup Shaw

Type-II seesaw model contains an $SU(2)_L$ triplet scalar field Δ with hypercharge $Y = 2$ in addition to the SM fields.

$$\Delta = \frac{\sigma^i}{\sqrt{2}}\Delta_i = \begin{pmatrix} \delta^+/\sqrt{2} & \delta^{++} \\ \delta^0 & -\delta^+/\sqrt{2} \end{pmatrix}, \quad (1)$$

where $\Delta_1 = (\delta^{++} + \delta^0)/\sqrt{2},\ \Delta_2 = i(\delta^{++} - \delta^0)/\sqrt{2},\ \Delta_3 = \delta^+$.
The complete Lagrangian of this scenario is given by:

$$\mathcal{L} = \mathcal{L}_{\mathrm{Yukawa}} + \mathcal{L}_{\mathrm{Kinetic}} - V(\Phi, \Delta), \quad (2)$$

where the kinetic and Yukawa interactions are respectively.

$$\mathcal{L}_{\mathrm{kinetic}} = (D_\mu\Phi)^\dagger (D^\mu\Phi) + \mathrm{Tr}\left[(D_\mu\Delta)^\dagger (D^\mu\Delta)\right], \quad (3)$$

$$\mathcal{L}_{\mathrm{Yukawa}} = \mathcal{L}^{\mathrm{SM}}_{\mathrm{Yukawa}} - (Y_\Delta)_{ij} L_i^T C i\sigma_2 \Delta L_j + \mathrm{h.c.} \quad (4)$$

Here $\Phi^T = (\phi^+ \quad \phi^0)$ is the SM scalar doublet.

$$D_\mu\Delta = \partial_\mu\Delta + i\frac{g}{2}[\sigma^a W^a_\mu, \Delta] + ig' B_\mu\Delta \qquad (a = 1, 2, 3). \quad (5)$$

The most general scalar potential[1] is given as :

$$V(\Phi,\Delta) = -m_\Phi^2(\Phi^\dagger\Phi) + \frac{\lambda}{4}(\Phi^\dagger\Phi)^2 + M_\Delta^2 \mathrm{Tr}(\Delta^\dagger\Delta) + \left(\mu\Phi^\mathsf{T} i\sigma_2\Delta^\dagger\Phi + \mathrm{h.c.}\right) -$$
$$\lambda_1(\Phi^\dagger\Phi)\mathrm{Tr}(\Delta^\dagger\Delta) + \lambda_2\left[\mathrm{Tr}(\Delta^\dagger\Delta)\right]^2 + \lambda_3\mathrm{Tr}(\Delta^\dagger\Delta)^2 + \lambda_4\Phi^\dagger\Delta\Delta^\dagger$$

After the EWSB, the minimization of the potential calculates the two mass parameters as,

$$m_\Phi^2 = \lambda\frac{v_d^2}{4} - \sqrt{2}\mu v_t + \frac{(\lambda_1+\lambda_4)}{2}v_t^2\,, \qquad (7)$$

$$M_\Delta^2 = \frac{\mu v_d^2}{\sqrt{2}v_t} - \frac{\lambda_1+\lambda_4}{2}v_d^2 - (\lambda_2+\lambda_3)v_t^2\,, \qquad (8)$$

The triplet vev (v_t) contributes to the electroweak gauge boson masses M_W^2 and M_Z^2 at tree level, $M_W^2 = \frac{g^2(v_d^2+2v_t^2)}{4}$ and $M_Z^2 = \frac{g^2(v_d^2+4v_t^2)}{4\cos^2\theta_W}$ respectively. The SM ρ-parameter is given by:

$$\rho = \frac{M_W^2}{M_Z^2\cos^2\theta_W} = \frac{1+\frac{2v_t^2}{v_d^2}}{1+\frac{4v_t^2}{v_d^2}}\,. \qquad (9)$$

[1] A. Arhrib et al,PhysRevD.84.095005

One gets an upper bound on $\frac{v_t}{v_d} < 0.02$ or $v_t < 5$ GeV.
After EWSB, the scalar fields expanded around respective vevs, can be parameterized as

$$\Phi = \frac{1}{\sqrt{2}} \begin{pmatrix} \sqrt{2}\chi_d^+ \\ v_d + h_d + i\eta_d \end{pmatrix} \qquad \Delta = \frac{1}{\sqrt{2}} \begin{pmatrix} \delta^+ & \sqrt{2}\delta^{++} \\ v_t + h_t + i\eta_t & -\delta^+ \end{pmatrix} \quad (10)$$

As a consequence, the scalar spectrum contains seven physical Higgs bosons: two doubly charged $H^{\pm\pm}$, two singly charged $H^{\pm}$, two CP-even neural (h, H) and a CP-odd (A) Higgs particles.
The corresponding mixing angles are given as

$$\tan\beta' = \frac{\sqrt{2}v_t}{v_d}, \quad \tan\beta = \frac{2v_t}{v_d} \equiv \sqrt{2}\tan\beta'$$

$$\text{and} \quad \tan 2\alpha = \frac{2\mathcal{B}}{\mathcal{A} - \mathcal{C}},$$

$$\text{where,} \quad \mathcal{A} = \frac{\lambda}{2}v_d^2, \qquad \mathcal{B} = v_d[-\sqrt{2}\mu + (\lambda_1 + \lambda_4)v_t], \quad \mathcal{C} = \frac{\sqrt{2}\mu v_d^2 + 4(\lambda_2 +}{2v_t}$$

- The scalar potential : 8 independent parameters.
- Minimization condition $\rightarrow$ m_Φ^2 and M_Δ^2 can be traded off for the two vevs (v_d, v_t).
- The remaining 5 scalar quartic couplings and μ-parameter can be expressed in terms of the 5-scalar masses and the neutral scalar mixing angle α.
- v_d and $m_h = 125$ GeV are known.
- Free parameters : $(m_H, m_A, m_H^{\pm}, m_{H^{\pm\pm}}, \alpha)$.

$$\lambda = \frac{2}{v_d^2}(c_\alpha^2 m_h^2 + s_\alpha^2 m_H^2)\,, \tag{12a}$$

$$\lambda_1 = \frac{4m_{H^\pm}^2}{v_d^2+2v_t^2} - \frac{2m_A^2}{v_d^2+4v_t^2} + \frac{\sin 2\alpha}{2v_d v_t}(m_h^2 - m_H^2)\,, \tag{12b}$$

$$\lambda_2 = \frac{1}{v_t^2}\left[\frac{1}{2}\left(s_\alpha^2 m_h^2 + c_\alpha^2 m_H^2\right) + \frac{1}{2}\frac{v_d^2 m_A^2}{v_d^2+4v_t^2} - \frac{2v_d^2 m_{H^\pm}^2}{v_d^2+2v_t^2} + m_{H^{\pm\pm}}^2\right]\,, \tag{12c}$$

$$\lambda_3 = \frac{1}{v_t^2}\left[\frac{2v_d^2 m_{H^\pm}^2}{v_d^2+2v_t^2} - m_{H^{\pm\pm}}^2 - \frac{v_d^2 m_A^2}{v_d^2+4v_t^2}\right]\,, \tag{12d}$$

$$\lambda_4 = \frac{4m_A^2}{v_d^2+4v_t^2} - \frac{4m_{H^\pm}^2}{v_d^2+2v_t^2}\,, \tag{12e}$$

$$\mu = \frac{\sqrt{2}v_t m_A^2}{v_d^2+4v_t^2}\,. \tag{12f}$$

To have the scalar potential to be bounded from below in all direction in field space, the following necessary and sufficient conditions on the scalar quartic couplings has to be satisfied.[2]

$$\begin{aligned}
\lambda &\geq 0\,, && (13a)\\
\lambda_2+\lambda_3 &\geq 0\,, && (13b)\\
\lambda_2+\frac{\lambda_3}{2} &\geq 0, && (13c)\\
\lambda_1+\sqrt{\lambda(\lambda_2+\lambda_3)} &\geq 0\,, && (13d)\\
\lambda_1+\sqrt{\lambda\left(\lambda_2+\frac{\lambda_3}{2}\right)} &\geq 0, && (13e)\\
\lambda_1+\lambda_4+\sqrt{\lambda(\lambda_2+\lambda_3)} &\geq 0\,, && (13f)\\
\lambda_1+\lambda_4+\sqrt{\lambda\left(\lambda_2+\frac{\lambda_3}{2}\right)} &\geq 0. && (13g)
\end{aligned}$$

[2] A. Arhrib etal, PRD 84, 095005 (2011).

Tree-level unitarity of the scattering amplitude for all $2 \to 2$ processes demands the S-matrix eigen-values to be bounded from above as below [3]:

$$
\begin{aligned}
|\lambda_1 + \lambda_4| &\leq 16\pi, && (14a)\\
|\lambda_1| &\leq 16\pi, && (14b)\\
|2\lambda_1 + 3\lambda_4| &\leq 32\pi, && (14c)\\
|\lambda| &\leq 32\pi, && (14d)\\
|\lambda_2| &\leq 8\pi, && (14e)\\
|\lambda_2 + \lambda_3| &\leq 8\pi, && (14f)\\
\left|\lambda + 4\lambda_2 + 8\lambda_3 \pm \sqrt{(\lambda - 4\lambda_2 - 8\lambda_3)^2 + 16\lambda_4^2}\right| &\leq 64\pi, && (14g)\\
\left|3\lambda + 16\lambda_2 + 12\lambda_3 \pm \sqrt{(3\lambda - 16\lambda_2 - 12\lambda_3)^2 + 24(2\lambda_1 + \lambda_4)^2}\right| &\leq 64\pi, && (14h)\\
|2\lambda_1 - \lambda_4| &\leq 16\pi, && (14i)\\
|2\lambda_2 - \lambda_3| &\leq 16\pi && (14j)
\end{aligned}
$$

[3] A. Arhrib etal, PRD 84, 095005 (2011)

- Constraints from electroweak precision test: The strongest bound comes from the T-parameter which imposes strict limit on the mass splitting between the doubly and singly charged scalars, $\Delta M \equiv \mid m_{H^{\pm\pm}} - m_{H^{\pm}} \mid$ which should be $\lesssim$ 50 GeV[4].
- The direct search on the singly charged scalar at the LEP II puts a limit on $m_{H^{\pm}} \geq 78$ GeV.
- The doubly charged scalars can either decay into $\ell^{\pm}\ell'^{\pm}$ or $W^{\pm}W^{\pm}$ (assuming degenerate heavy scalars).
- $\Gamma(H^{++} \to \ell_i^+ \ell_j^+) = \frac{m_{H^{++}}}{8\pi(1+\delta_{ij})} \left[Y_{ij}\right]^2$;
- $\Gamma(H^{++} \to W^+ W^+) = \frac{g^4 v_t^2}{8\pi m_{H^{++}}} \sqrt{(1 - \frac{4M_W^2}{m_{H^{++}}^2})} \left[2 + \left(\frac{m_{H^{++}}^2}{2M_W^2} - 1\right)^2\right]$.
- For $v_t < 10^{-4}$ GeV (corresponds to large Yukawa couplings) and assuming degenerate scalars, the doubly charged Higgs boson decays to like sign dilepton (LSD) $\ell^{\pm}\ell^{\pm}$ with almost 100% probability. From the direct search of the doubly charged Higgs boson at $\sqrt{s} = 13$ TeV with 36.1 fb^{-1} data at the LHC, the current lower bound at 95% CL on its mass is $m_{H^{\pm\pm}} > 700 - 850$ GeV[5] depending upon the final state lepton flavor.

---

[4] E. J. Chun et al.,JHEP11(2012)106

[5] ATLAS collaboration, arXiv:1710.09748

- For our choice of benchmark points, $m_{H^\pm} \sim 173 - 180$ GeV and for this mass range, the $t \to bH^+$ decay mode is kinematically suppressed.
- At the LHC $gg \to \Phi$, $(\Phi \equiv H/A)$ is the dominant production mode. For Type II Seesaw model, interactions between quarks and $SU(2)_L$ triplet scalars happen via the $SU(2)_L$ doublet (SM like Higgs boson) and triplet mixing, which is proportional to (v_t/v_d).
- For our choice of the triplet vev $(v_t = 3\ \mathrm{GeV})$, the $\sigma(pp(gg) \to H) \propto (v_t/v_d)^2 \sim \mathcal{O}(10^{-4}) \Longrightarrow \sigma(pp \to H) \approx 13$(fb) for the best possible scenario and this is well below the 95% CL bound on $\sigma(gg \to H) \times \mathrm{BR}(H \to ZZ)$ $(pb) - m_H$ plane by the ATLAS collaboration[6].
- For $v_t = 3$ GeV, $H^{\pm\pm} \to W^\pm W^\pm, W^\pm H^\pm, H^\pm H^\pm$ if kinematically accessible.
- Due to the cascade nature of the final state, the collider bound on the $H^{\pm\pm}$ in this case is rather weak.
- Our choice of benchmark points remain within the 2σ limit of the current experimental bound $(0.85^{+0.22}_{-0.20})$ of the Higgs to diphoton signal strength.

[6] ATLAS-CONF-2016-016, 2016

- We look for the collider signature of the associated production of singly and doubly charged scalars.
- Depending upon the mass hierarchy, we can have two scenarios :
  - Positive scenario ($\lambda_4 > 0$) :: $m_{H^{\pm\pm}} < m_{H^{\pm}} < m_A/m_H$
  - Negative scenario ($\lambda_4 < 0$) :: $m_{H^{\pm\pm}} > m_{H^{\pm}} > m_A/m_H$
- We choose $v_t = 3$ GeV $\Longrightarrow H^{\pm\pm} \to \ell^{\pm}\ell^{\pm}$ extremely suppressed and only decay to gauge bosons are allowed.
- At such value, $\mathrm{Br}(H^{\pm\pm} \to W^{\pm}W^{\pm}) \simeq 100\%$ while the singly charged scalar can have mainly three types of decays : $W^{\pm}Z, t\bar{b}, W^{\pm}h$ depending upon the phase space available.

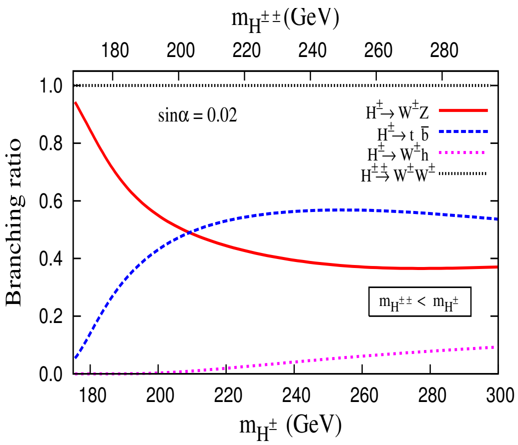

$m_{H^{\pm\pm}}$ (GeV)
180
200
220
240
260
280
1.0
0.8
0.6
0.4
0.2
0.0
Branching ratio
sinα = 0.02
$H^{\pm} \to W^{\pm}Z$
$H^{\pm} \to t\ \bar{b}$
$H^{\pm} \to W^{\pm}h$
$H^{\pm\pm} \to W^{\pm}W^{\pm}$
$m_{H^{\pm\pm}} < m_{H^{\pm}}$
180
200
220
240
260
280
300
$m_{H^{\pm}}$ (GeV)

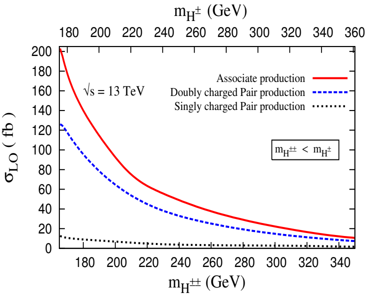

Figure: *Left (Right) panel shows the variation of* $\sigma_{\rm LO}(pp \to H^{\pm\pm}H^{\mp})$ (fb) *(solid red curve),* $\sigma_{\rm LO}(pp \to H^{++}H^{--})$ (fb) *(blue dashed curve) and* $\sigma_{\rm LO}(pp \to H^{+}H^{-})$ (fb) *(black dotted curve) with respect to charged Higgs masses at the LHC at* $\sqrt{s} = 13$ TeV *for positive (negative) scenario.*

Mass Scenario	$\sin\alpha$	$m_{H^{\pm\pm}}$ (GeV)	$m_{H^{\pm}}$ (GeV)	$m_H = m_A$ (GeV)	$\mu_{\gamma\gamma}$
Positive					
BP1	0.0220	165.48	173.25	180.70	0.79
BP2	0.0280	175.99	177.47	178.93	0.82
Negative					
BP1	0.0277	179.60	176.30	173.01	0.79
BP2	0.0300	184.17	180.11	175.95	0.81

Table: *Benchmark points valid by the high-scale stability constraints up to the Planck scale and their corresponding Higgs to diphoton signal strength ($\mu_{\gamma\gamma}$) for both the positive and the negative scenario.*

.

We consider the following two signal topologies:

$$(i) \quad 3\ell^{\pm} + \not{E}_T;$$
$$(ii) \quad (\ell^{+}\ell^{+}) + 4j + \not{E}_T,$$

SM background processes : $t\bar{t}$+jets (up to 3), single top with three hard jets, $V + \text{jets (up to 3 jets)}$, $V \equiv W^{\pm}, Z$, $VV+$ 3 jets, $t\bar{t} + (W^{\pm}/Z/h)$, and VVV.

In our signal and background events, we select jets and leptons using the following basic kinematical acceptance cuts :

$$\Delta R_{jj} > 0.6, \quad \Delta R_{\ell\ell} > 0.4, \quad \Delta R_{j\ell} > 0.7\,, \tag{15a}$$

$$\Delta R_{bj} > 0.7, \quad \Delta R_{b\ell} > 0.2, \tag{15b}$$

$$p^{j}_{T_{\min}} > 20\ \mathrm{GeV}, \quad |\eta_j| < 5, \tag{15c}$$

$$p^{\ell}_{T_{\min}} > 10\ \mathrm{GeV}, \quad |\eta_\ell| < 2.5, \tag{15d}$$

b-jet abiding by the efficiency as proposed by the ATLAS collaboration:

$$\epsilon_b = \begin{cases} 0 & p_T^b \leq 30\ \mathrm{GeV} \\ 0.6 & 30\ \mathrm{GeV} < p_T^b < 50\ \mathrm{GeV} \\ 0.75 & 50\ \mathrm{GeV} < p_T^b < 400\ \mathrm{GeV} \\ 0.5 & p_T^b > 400\ \mathrm{GeV}\ . \end{cases} \tag{16}$$

$$pp \to H^{++}H^{-} \to (W^{+}W^{+}) + (W^{-}Z) \to (\ell^{+}\ell^{+}) + \ell^{-} + \not{E}_T.$$

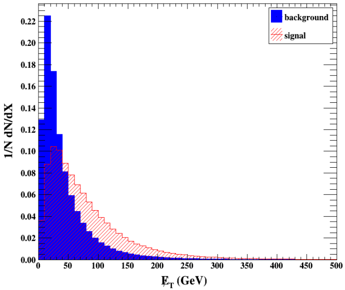

Figure: *Normalized distribution of the (left panel) Missing transverse energy ($\not{E}_T$) and (right panel) the transverse momentum of the hardest lepton ($p_T(\ell_1)$) after the basic kinematical acceptance cuts for the benchmark BP1 of positive scenario.*

$3\ell^{\pm} + \not{E}_T$

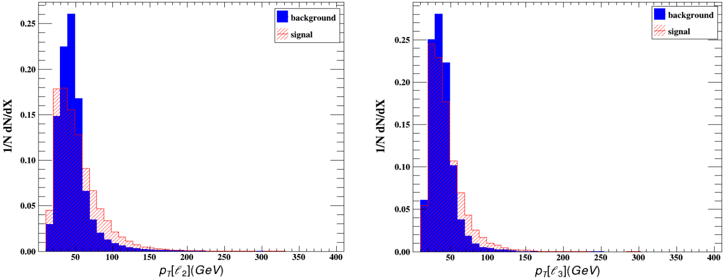

Figure: *Transverse momentum (p_T) distribution (normalized) of the two sub-leading leptons for the benchmark BP1 of positive scenario.*

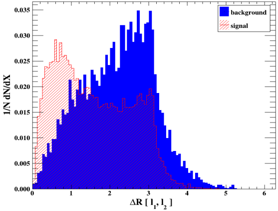

Figure: *The $\Delta R(\ell_1^{\pm}\ell_2^{\pm})$ distribution (normalized) between the two same-sign leptons for the positive scenario benchmark BP1.*

- (**C1-1**): Our signal event is hadronically quiet, hence, we put a veto on any jet with $p_T > 30$ GeV.
- (**C1-2**): Next, to confirm the trilepton signature, we select at least three leptons with $p_T > 10$ GeV.
- (**C1-3**): For further affirmation of trilepton signature, we reject any additional charged lepton with $p_T > 10$ GeV.
- (**C1-4**): $\mid \mathrm{M}_{\ell^+\ell^-} - M_Z \mid > 10$ GeV, to ensure that those are not directly produced from Z boson.

- (**C1-5**): Finally, our signal events are required to have $\not{E}_T > 30$ GeV.
- (**C1-6**): The principal selection cut for the same-sign dilepton has been imposed. For this, we demand $\Delta R(\ell_1^\pm \ell_2^\pm) < 1.5$.

SM-background	Production Cross section (fb)	Effective cross section (fb) for background after the cut C1–1	C1–2	C1–3	C1–4	C1–5	C1–6	
t+jets	2.22×10^5	157.50	0	0	0	0	0	
$t\bar{t}$+jets	7.07×10^5	420.37	0	0	0	0	0	
$W^\pm$+jets	1.54×10^8	4.96×10^7	0	0	0	0	0	
Z+jets	4.54×10^7	1.37×10^7	0	0	0	0	0	
W^+W^-+jets	8.22×10^4	4.76×10^3	0	0	0	0	0	
ZZ+jets	1.10×10^4	6.17×10^2	10.05	5.77	0.08	0.04	~ 0	
$W^\pm Z$+jets	3.81×10^4	1.71×10^3	42.40	42.40	0.72	0.36	0.04	
W^+W^-Z	83.10	1.17	0.09	0.07	0.01	~ 0	0	
$W^\pm ZZ$	26.80	0.39	0.03	0.03	~ 0	0	0	
$t\bar{t} + W^\pm$	360	0.13	0.02	~ 0	0	0	0	
$t\bar{t} + Z$	585	0.15	0.02	0.01	~ 0	0	0	
$t\bar{t} + h$	400	0.02	~ 0	0	0	0	0	
Total SM Background	2.005×10^8	6.33×10^7	52.60	48.30	0.81	0.40	0.04	
Positive scenario	Production Cross section (fb)	Effective cross section (fb) for signal after the cut						Luminosity (in fb^{-1}) for 5σ significance
BP1	185.10	0.75	0.20	0.14	0.08	0.06	0.040	1250.0
BP2	158.70	0.65	0.16	0.11	0.06	0.05	0.034	1600.4
Negative scenario	Production Cross section (fb)	Effective cross section (fb) for signal after the cut						Luminosity (in fb^{-1}) for 5σ significance
BP1	153.80	0.63	0.16	0.11	0.06	0.05	0.033	1675.8
BP2	134.70	0.55	0.15	0.10	0.05	0.04	0.030	1944.4

Table: *Effective cross section obtained after each cut for both signal ($3\ell^\pm + \not{E}_T$) and background and the respective required integrated luminosity for* 5σ significance at 13 TeV LHC.

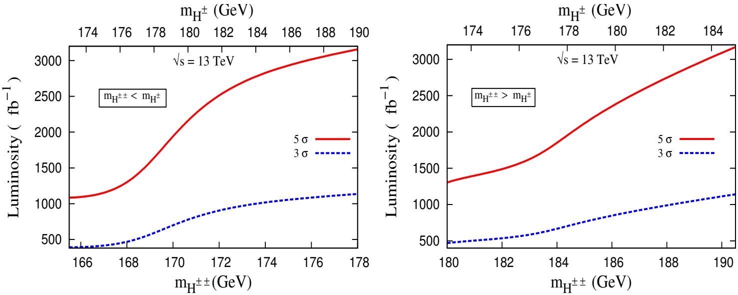

Figure: *Left (Right) panel shows the required integrated luminosity for* $3\ell^{\pm} + \not{E}_T$ *final state with respect to charged Higgs masses at the LHC at* $\sqrt{s} = 13$ TeV *for positive (negative) scenario. The solid red coloured and blue coloured dashed curve correspond to constant signal significance at* 5σ and 3σ respectively.

$2\ell^{\pm} + 4j + \not{E}_T$

$$
\begin{aligned}
pp \to H^{++}H^{--} &\to (W^+W^+) + (W^-W^-) \to (\ell^+\ell^+) + 4j + \not{E}_T \\
pp \to H^{++}H^{-} &\to (W^+W^+) + (W^-Z) \to (\ell^+\ell^+) + 4j + \not{E}_T \,. (17)
\end{aligned}
$$

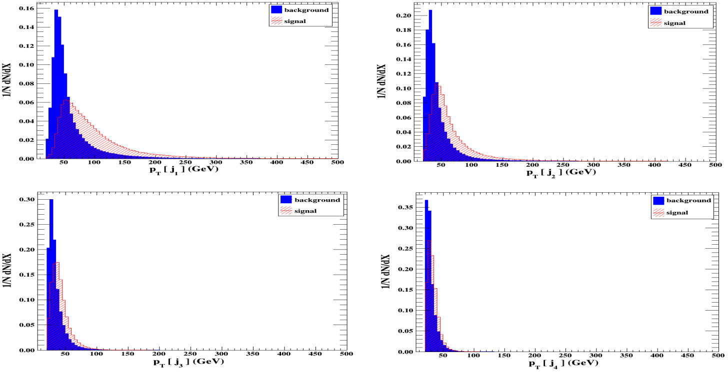

Figure: *Transverse momentum (p_T) distribution (normalized) of the four leading jets for the final state $2\ell^{\pm} + 4j + \not{E}_T$ for the benchmark BP1 of positive scenario.*

- (**C2-1**): As explained, our signal is exempted from any b-jets, hence we can safely reject events with b-tagged jets of $p_T(b) > 40$ GeV.
- (**C2-2**): To guarantee that only 4 jets are present in the events, we reject any additional jets with $p_T(j_5) > 20$ GeV.
- (**C2-3**): Our signal also contains two isolated charged lepton and thus a veto on any additional leptons with $p_T > 10$ GeV is applied.
- (**C2-4**): Now, from the jet distribution, we choose the p_T of the leading jet to be at least greater than $p_T(j_1) > 60$ GeV.
- (**C2-5**): Moreover, for the next sub-leading jet we demand $p_T(j_2) > 40$ GeV to further subdue the background events.

- (**C2-6**): A decent selection cut on the missing transverse energy is then applied as $\not{E}_T > 30$ GeV.
- (**C2-7**): Finally, the principal selection cut for the same-sign dilepton has been imposed. For this, we demand $\Delta R(\ell_1^{\pm}\ell_2^{\pm}) < 1.5$.

		Effective cross section (fb) after the cut							
SM-background	Production Cross section (fb)	C2–1	C2–2	C2–3	C2–4	C2–5	C2–6	C2–7	
t+jets	2.22×10^5	8.46×10^4	8.01×10^4	8.01×10^4	4.89×10^4	3.44×10^4	1.54×10^4	0	
$t\bar{t}$+jets	7.07×10^5	1.58×10^5	1.23×10^5	1.23×10^5	9.92×10^4	8.15×10^4	5.58×10^4	0	
$W^{\pm}$+jets	1.54×10^8	1.52×10^8	1.52×10^8	1.52×10^8	1.24×10^7	8.17×10^6	1.75×10^6	0	
Z+jets	4.54×10^7	4.27×10^7	4.27×10^7	4.27×10^7	3.76×10^6	2.48×10^6	4.65×10^5	0	
W^+W^-+jets	8.22×10^4	7.84×10^4	7.55×10^4	7.55×10^4	3.48×10^4	2.39×10^4	1.04×10^4	0	
ZZ+jets	1.10×10^4	8.96×10^3	8.67×10^3	8.65×10^3	4.27×10^3	2.89×10^3	1.16×10^3	0.05	
$W^{\pm}Z$+jets	3.81×10^4	3.33×10^4	3.13×10^4	3.12×10^4	1.67×10^4	1.18×10^4	5.76×10^3	1.68	
$t\bar{t} + W^{\pm}$	360	78.00	55.15	55.00	47.00	39.80	33.00	0.13	
$t\bar{t} + Z$	585	110.00	68.20	67.00	59.60	52.04	44.30	0.04	
$t\bar{t} + h$	400	46.00	27.40	27.20	24.50	21.65	18.30	0.04	
Total SM Background	2.005×10^8	1.95×10^8	1.94×10^8	1.94×10^8	1.64×10^7	1.08×10^7	2.31×10^6	1.94	
Positive scenario	Production Cross section (fb)	Effective cross section (fb) for signal after the cut							Luminosity (in fb^{-1}) for 5σ significance
BP1	311.40	253.00	210.70	206.70	181.72	158.90	126.24	1.90	26.6
BP2	259.30	211.23	175.92	172.64	151.75	132.66	105.42	1.55	36.3
Negative scenario	Production Cross section (fb)	Effective cross section (fb) for signal after the cut							Luminosity (in fb^{-1}) for 5σ significance
BP1	246.23	200.00	166.50	163.32	143.61	125.54	99.76	1.50	38.2
BP2	219.30	177.74	148.03	145.22	127.70	111.63	88.71	1.30	47.9

Table: *Effective cross section obtained after each cut for both signal ($2\ell^{\pm} + 4j + \not{E}_T$) and background and the respective required integrated luminosity for* 5σ significance at 13 TeV LHC.

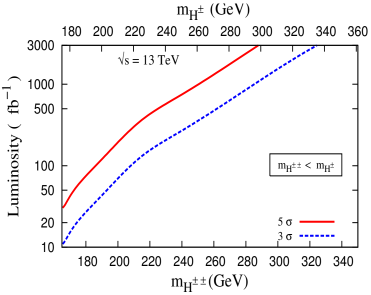

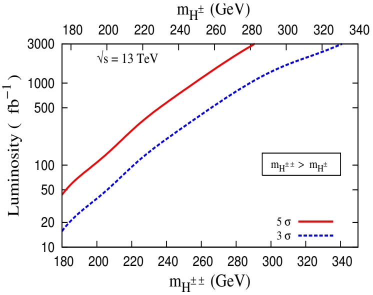

Figure: *Left (Right) panel shows the required integrated luminosity for $2\ell^{\pm} + 4j + \not{E}_T$ final state with respect to charged Higgs masses at the LHC at $\sqrt{s} = 13$ TeV for positive (negative) scenario.*

- Type II Seesaw model is one of the very popular scenario to give mass to neutrinos.
- Model contains one complex $SU(2)_L$ triplet scalar field.
- We have considered the triplet vev $v_t = 3$ GeV.
- We have non-degenerate mass scenario.
- Depending on the mass hierarchy, two possible scenarios (positive and negative) exist which however, at the end, yielded similar signal significance. In the allowed parameter space, with appreciable production cross section, the masses of the charged scalar can presumably be chosen around 200 GeV.
- Two specific final states at the collider, $(3\ell^{\pm} + \not{E}_T)$ and $(2\ell^{\pm} + 4j + \not{E}_T)$ at the 13 TeV LHC run. A proper cut-based analysis with detector simulation reveals that the first channel can only be probed at the 13 TeV LHC with high integrated luminosity around $1200\ \mathrm{fb}^{-1}$ and should be promoted for a HL-LHC. On the other hand, for the second channel we have found that even a 5σ discovery reach is possible with the present LHC data with only around 40 fb^{-1} luminosity.


Thank you!!

Here, we will present the one loop RGEs of all the relevant couplings (gauge, Yukawa and scalar quartic couplings) of the Type-II seesaw model[M. A. Schmidt et at, PhysRevD.76.073010]. For convenience, we introduce the shorthand notation $\mathcal{D} \equiv 16\pi^2 \frac{\mathrm{d}}{\mathrm{d}(\ln\mu)}$.

Gauge and top Yukawa couplings: The RGE for the gauge couplings,

$$\mathcal{D}g_1 = \frac{47}{10}{g_1}^3 \,, \tag{18a}$$

$$\mathcal{D}g_2 = -\frac{5}{2}g_2^3 \,, \tag{18b}$$

$$\mathcal{D}g_3 = -7g_3^3 \,. \tag{18c}$$

The RGE for the top Yukawa coupling,

$$\mathcal{D}y_t = y_t\left(\frac{9}{2}y_t^2 - \left(8g_3^2 + \frac{9}{4}g_2^2 + \frac{17}{20}{g_1}^2\right)\right) \,, \tag{18d}$$

where, $g_1 = \sqrt{\frac{5}{3}}g'$ with GUT renormalization.

Scalar quartic couplings: We express the RGEs of the scalar quartic coupling with a redefinition of the coupling to match with the potential notation of Ref. [**?**] which can be translated from our notation in the following way.

$$
\begin{aligned}
\Lambda_0 &= \frac{\lambda}{2}\,, && (19a)\\
\Lambda_1 &= 2\lambda_2 + 2\lambda_3\,, && (19b)\\
\Lambda_2 &= -2\lambda_3\,, && (19c)\\
\Lambda_4 &= \lambda_1 + \frac{\lambda_4}{2}\,, && (19d)\\
\Lambda_5 &= -\frac{\lambda_4}{2}\,. && (19e)
\end{aligned}
$$

The RGEs for the five quartic couplings that appear are then given by,

$$\mathcal{D}\Lambda_i = \beta_{\Lambda_i} + G_i\,, (i = 0, 1, 2, 4, 5)\,, \tag{20}$$

where, β_{Λ_i} and G_i are as follows:

$$
\begin{aligned}
\beta_{\Lambda_0} &= 12\Lambda_0^2 + 6\Lambda_4^2 + 4\Lambda_5^2\,, && (21a)\\
\beta_{\Lambda_1} &= 14\Lambda_1^2 + 4\Lambda_1\Lambda_2 + 2\Lambda_2^2 + 4\Lambda_4^2 + 4\Lambda_5^2\,, && (21b)\\
\beta_{\Lambda_2} &= 3\Lambda_2^2 + 12\Lambda_1\Lambda_2 - 8\Lambda_5^2\,, && (21c)\\
\beta_{\Lambda_4} &= \Lambda_4\left(8\Lambda_1 + 2\Lambda_2 + 6\Lambda_0 + 4\Lambda_4 + 8\Lambda_5^2\right)\,, && (21d)\\
\beta_{\Lambda_5} &= \Lambda_5\left(2\Lambda_1 - 2\Lambda_2 + 2\Lambda_0 + 8\Lambda_4\right)\,, && (21e)
\end{aligned}
$$

and,

$$G_0 = \left(12y_t^2 - \left(\frac{9}{5}g_1^2 + 9g_2^2\right)\right)\Lambda_0 + \frac{9}{4}\left(\frac{3}{25}g_1^4 + \frac{2}{5}g_1^2g_2^2 + g_2^4\right) - 12y_t^4 \tag{22a}$$

$$G_1 = -\left(\frac{36}{5}g_1^2 + 24g_2^2\right)\Lambda_1 + \frac{108}{25}g_1^4 + 18g_2^4 + \frac{72}{5}g_1^2g_2^2\,, \tag{22b}$$

$$G_2 = -\left(\frac{36}{5}g_1^2 + 24g_2^2\right)\Lambda_2 + 12g_2^4 - \frac{144}{5}g_1^2g_2^2\,, \tag{22c}$$

$$G_4 = \left(6y_t^2 - \left(\frac{9}{2}g_1^2 + \frac{33}{2}g_2^2\right)\right)\Lambda_4 + \frac{27}{25}g_1^4 + 6g_2^4\,, \tag{22d}$$

$$G_5 = \left(6y_t^2 - \left(\frac{9}{2}g_1^2 + \frac{33}{2}g_2^2\right)\right)\Lambda_5 - \frac{18}{5}g_1^2g_2^2\,. \tag{22e}$$

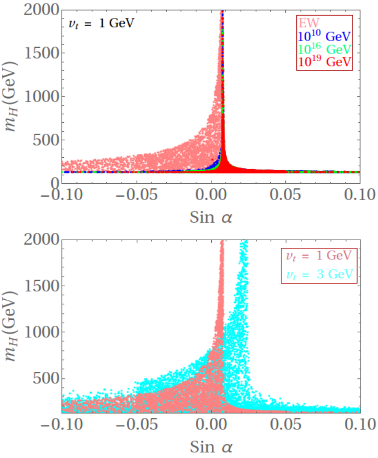

Figure: *(Upper panel) The valid parameter space in the* $\sin\alpha - m_H$ *plane for* $v_t = 1$ GeV *(left) and* $v_t = 3$ GeV *(right) for different values of cut-off scale.(Lower panel) The explicit distinction between the allowed parameter space by the two different* v_t *valid only at the EW scale(left) and all the way up to the Planck scale(right).*

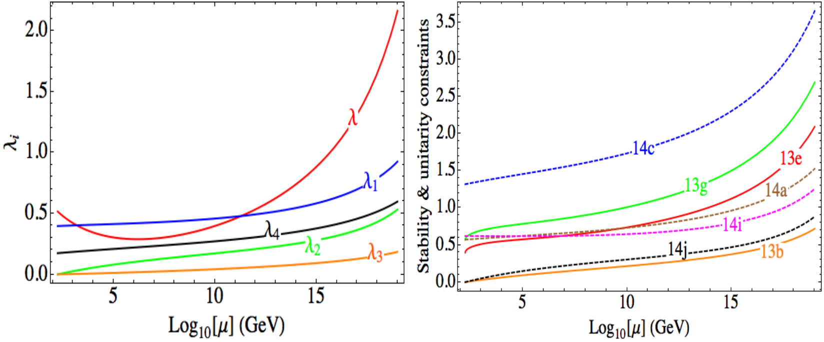

Figure: *(Left panel) The running of the five scalar quartic couplings up to the Planck scale for the benchmark point BP1 of positive scenario. (Right panel) The running of some of the stability and unitarity constraints indicated by the corresponding equation numbers for the same benchmark point.*

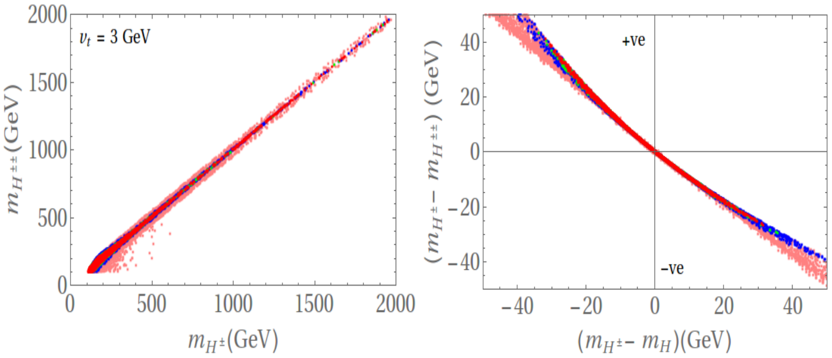

Figure: *(Left panel) The allowed parameter space in the $m_{H^\pm} - m_{H^{\pm\pm}}$ plane for triplet vev $v_t = 3\ \mathrm{GeV}$. The different colors follow the same convention as in Fig.* **??**. *(Right panel) The corresponding allowed parameter space to show the relation between the mass splittings of the singly charged Higgs to the neutral Higgs $(m_{H^\pm} - m_H)$ and singly charged Higgs to the doubly charged Higgs $(m_{H^\pm} - m_{H^{\pm\pm}})$. The upper left square corresponds to the valid region for our positive scenario while the lower right corner denotes the same but for our negative scenario.*